

Gene expression changes in a tumor xenograft by a pyrrole-imidazole polyamide

Jevgenij A. Raskatov^a, Nicholas G. Nickols^{a,b}, Amanda E. Hargrove^a, Georgi K. Marinov^c, Barbara Wold^c, and Peter B. Dervan^{a,1}

^aDivision of Chemistry and Chemical Engineering, California Institute of Technology, Pasadena, CA 91125; ^bDepartment of Radiation Oncology, David Geffen School of Medicine of the University of California Los Angeles, Los Angeles, CA 90095-6951; and ^cDivision of Biology, California Institute of Technology, Pasadena, CA 91125

Contributed by Peter B. Dervan, August 20, 2012 (sent for review July 10, 2012)

Gene regulation by DNA binding small molecules could have important therapeutic applications. This study reports the investigation of a DNA-binding pyrrole-imidazole polyamide targeted to bind the DNA sequence 5'-WGGWWW-3' with reference to its potency in a subcutaneous xenograft tumor model. The molecule is capable of trafficking to the tumor site following subcutaneous injection and modulates transcription of select genes in vivo. An FITC-labeled analogue of this polyamide can be detected in tumor-derived cells by confocal microscopy. RNA deep sequencing (RNA-seq) of tumor tissue allowed the identification of further affected genes, a representative panel of which was interrogated by quantitative reverse transcription-PCR and correlated with cell culture expression levels.

tumor RNA-sequencing | eXpress | in vivo circulation | efficacy

Pyrrole-imidazole (Py-Im) polyamides represent a class of modular DNA minor groove binders with affinity and specificity comparable to the values observed with typical DNA binding proteins (1, 2). Our previous investigations have established a framework for molecular recognition of the minor groove of DNA by polyamides that can target predetermined DNA binding sites (3–5). Cell culture experiments have shown that cellular uptake of Py-Im polyamides targeting six-base pair sequences can be observed (6). Subsequent studies demonstrated that Py-Im polyamides could antagonize DNA binding of transcription factors in live cells. Interrogated transcription factors include the androgen receptor (AR) (7), hypoxia inducible factor 1 alpha (HIF-1 α) (8), the glucocorticoid receptor (GR) (9), and nuclear factor kappa B (NF- κ B) (10).

Although there is more knowledge to be gained from deeper genome-wide cell culture studies, the next frontier for Py-Im polyamides as medicinally relevant small molecules lies in in vivo applications. Our recent studies demonstrated that the pharmacokinetics and toxicity of Py-Im polyamides in mice depend on architecture (11). Micromolar levels of compounds were observed in mouse plasma for up to 48 h following either intraperitoneal (i.p.) or subcutaneous (s.c.) injection. Efforts of Nagashima et al. established that Py-Im polyamides of different architecture were detectable in rat serum several hours after intravenous (i.v.) administration (12). Matsuda et al. further showed that a Py-Im polyamide targeted to the TGF- β 1 promoter affected target gene expression in vivo (rat renal cortex) without evidence of systemic toxicity (13, 14). The present study focuses on the question of whether Py-Im polyamides affect gene expression in vivo, specifically in a xenograft model environment, employing a luciferase-expressing derivative of the commonly used lung nonsmall cell carcinoma line A549.

Results

Acetylated Py-Im Polyamide 1 is More Potent in Cell Culture Than the Analog 2. The first set of experiments compared the in vitro gene regulation activity of Py-Im polyamides **1** and **2**, both targeted to bind to the sequence 5'-WGGWWW-3' (Fig. 1A). Our previous

efforts established that the polyamide **2** was capable of modulating a subset of TNF-inducible genes (10). Among the strongly affected genes we had identified *CCL2* and *SERPINE1* as highly repressed targets of **2**.

The basal expression levels of *CCL2* and *SERPINE1* were sufficiently high to enable the study of polyamide effects in the uninduced state. We found that both **1** and **2** reduced the levels of the two transcripts, but the effects exerted by **1** were substantially more pronounced (Fig. 1B). In line with the previous study, prolonged incubation times resulted in stronger down-regulation of the target genes—up to fivefold with *CCL2* and 14-fold with *SERPINE1*. Furthermore, **1** was significantly more cytotoxic in vitro than **2** against the chosen cell line with IC₅₀ values of 13 \pm 5 μ M and 33 \pm 2 μ M, respectively (SI Text, Fig. S1A). The more potent Py-Im polyamide **1** was, therefore, chosen for in vivo gene regulation experiments. Cellular uptake measurements clearly showed that the FITC-labeled analogue **3** was readily taken up by A549-luc-C8 cells, resulting in characteristic nuclear fluorescence (SI Text, Fig. S1B).

Py-Im Polyamides 1 and 2 Reach Comparable Plasma Levels with Similar Circulation Times Following S.C. Injection. Prior to conducting in vivo tumor xenograft experiments the pharmacokinetic profiles of **1** and **2** were compared. Our previous investigations showed that **2** could circulate in wild-type mice for several hours at micromolar plasma concentrations but dropped below the limit of detection after 24 h (11). The compound was administered by either the s.c. or the i.p. route and blood collected retro-orbitally. The circulation experiment was conducted for the Py-Im polyamide **1** using subcutaneous administration conditions analogous to those previously reported for **2**. The observed plasma levels compared well with those reported for **2** (Fig. 2 and Fig. S2). Maximum plasma concentrations of 10 μ M were attained for both compounds 3 h post injection. The plasma elimination phase appeared slightly shallower for the acetylated Py-Im polyamide **1** than for its close analog **2**, but neither was detectable 24 h post injection.

FITC-Labeled Py-Im Polyamide 3 Can Be Detected in Xenograft-Derived Cell Nuclei. We proceeded to synthesize the fluorescently tagged derivative of **1**, Py-Im polyamide **3** (see SI Text, Fig. S1 for structure). Previous experiments had shown that a closely related compound was stable in vivo and circulated in mice for several

Author contributions: J.A.R., and P.B.D. designed research; J.A.R., N.G.N., and A.E.H. performed research; J.A.R., N.G.N., A.E.H., G.K.M., B.W., and P.B.D. analyzed data; and J.A.R., and P.B.D. wrote the paper.

The authors declare no conflict of interest.

Freely available online through the PNAS open access option.

Data deposition: The data reported in this paper have been deposited in the Gene Expression Omnibus (GEO) database, www.ncbi.nlm.nih.gov/geo (accession no. GSE40218).

¹To whom correspondence should be addressed. E-mail: dervan@caltech.edu.

This article contains supporting information online at www.pnas.org/lookup/suppl/doi:10.1073/pnas.1214267109/-DCSupplemental.

10 μM were attainable for several hours post injection, it was conceivable that **1** could affect tumor growth. Tumor size was therefore assessed by luciferase imaging as outlined in *Materials and Methods*. A linear correlation between tumor size and photon number over several orders of magnitude has been previously demonstrated for the cell line used (www.caliperls.com/assets/018/7635.pdf). The luciferase output remained within experimental error between the two groups, suggesting that the gene expression changes did not stem from cytotoxicity (*SI Text*, Fig. S3).

Genome-Wide Effects of the Py-Im Polyamide 1. In order to establish the global effects of **1** in a xenograft setting, we measured changes in gene expression using RNA-seq in tumors from treated and untreated mice (see *Materials and Methods* for details). As our RNA-seq libraries contained a mixture of human and mouse RNA derived from the xenograft as well as the host cells infiltrating it, we faced the challenge of accurately determining the transcripts and genes from which sequencing reads originate (*Table S2* and discussion in the *SI Text*). We therefore designed an analysis pipeline based upon mapping reads to a combined human and mouse transcriptome and using the recently developed eXpress software package (bio.math.berkeley.edu/eXpress/index.html) to quantify probabilistically transcript abundance for both species simultaneously (Fig. 4). The eXpress output was used as input for differential expression analysis using DESeq (16).

Out of 22,092 genes, 618 (2.8%) experienced a statistically significant change in expression at a confidence level of $p < 0.05$. Within this subpopulation, 115 (0.52%) genes were repressed at least twofold, whereas 53 genes (0.24%) showed at least a twofold up-regulation. For quality control purposes, one replicate was resequenced using paired-end read sequencing with the read length set at 100 nt. High correlation coefficients were determined between the effective counts obtained by single- and paired-end read sequencing, with R^2 values of 0.97 and 0.94 for vehicle and **1**, respectively (see *SI Text*, Fig. S4 for correlation plots).

Comparison of RNA-seq and qRT-PCR for a Panel of Selected Genes in Vivo. A representative panel of genes studied by RNA-seq was further interrogated by qRT-PCR (Fig. 5, *Upper* and *Table 1*). In addition to *CCL2* and *SERPINE1* that were discussed above, we investigated the effects of **1** on transcription of *NPTX1*, *ROBO1*, *ATM*, *EGFR*, and *MMP28*. The genes were selected so as to range from strongly repressed (*NPTX1*) through weakly down-regulated (*ATM* and *EGFR*) to up-regulated upon polyamide treatment (*MMP28*). *NPTX1* experienced a 3.3-fold repression upon treatment with **1**, whereas the expression of *ATM* was reduced only 1.5-fold. The expression changes in *EGFR* detected by qPCR lie close to the error of the experiment (1.2-fold down). The expression of *MMP28* on the other hand was up-regulated 1.5-fold upon treatment with the Py-Im polyamide **1**. The genes *CCL2*, *NPTX1*, *SERPINE1*, and *MMP28* were categorized as differentially expressed by both techniques (*Table 1*). Changes in expression of *ATM* and *ROBO1* were only statistically significant assessed by qRT-PCR, not by RNA-seq (p -values over 0.05)

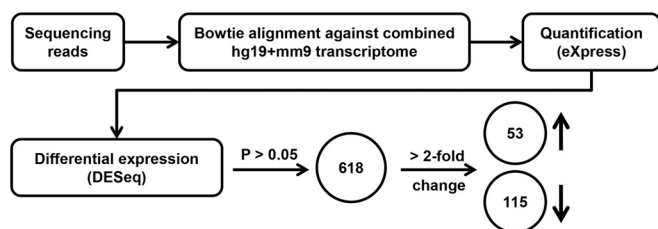


Fig. 4. Schematic representation of the pipeline for RNA-seq analysis of tumor-derived RNA. Three independent experiments for each of which $N = 5$ animals per treatment condition (vehicle vs **1**) were averaged, were jointly analyzed.

Comparison of in Vivo and in Vitro Effects of 1 by qRT-PCR on a Panel of Selected Genes. The gene expression changes in the in vivo xenograft setting were compared to those observed in cell culture (Fig. 5, *Lower* and *Table S3*). Prolonged incubation with Py-Im polyamide **1** in cell culture generally led to more pronounced effects (48 h vs 72 h), the only exception being *MMP28*, for which no effect was observed in cell culture regardless of the incubation time. The correspondence between the in vivo experiment and the cell culture control was found to depend strongly on the transcript interrogated. The in vitro effect of **1** on *NPTX1* expression at 72 h incubation was very close to that observed in vivo (3.5-fold vs 3.3-fold), whereas for *CCL2* the gene repression in xenografts resembled more closely the 48 h incubation time point from cell culture experiments (2.3-fold vs 2.2-fold). While *MMP28* expression was unchanged in cell culture, all other interrogated genes were affected more strongly than in the xenograft setting. The largest difference was noted for *SERPINE1*, which was repressed 2.0-fold in vivo but experienced a down-regulation in cell culture amounting to as much as 15.7-fold.

Discussion

The present study shows that the polyamide **1** is capable of trafficking to a xenografted tumor and yielding measurable gene expression changes. Following the establishment of pharmacokinetic properties of Py-Im polyamides targeted to the sequence 5'-WGGWW-3' (11), this is the next important step towards the application of Py-Im polyamides in a setting relevant to disease.

Comparison Between Xenografts and Cell Culture. Quantitative correlation between the two settings is of high interest, but differences in exposure times and concentrations of the Py-Im polyamide **1** between cell culture and at the tumor site need to be kept in mind. Typical exposure times in cell culture range from 48 h to 72 h whereas final treatment concentrations do not exceed 10 μM (10). Most of the polyamide remains in the medium so that the concentration is effectively invariant over the experimental time-course. One fundamental difference in the in vivo experiment is that the serum concentration of **1** does change as a function of postinjection time. Whereas a concentration maximum of approximately 10 μM is typically attained under chosen administration conditions, the circulating levels of **1** drop below the level of detection (high nanomolar) 24 h postinjection. This results in oscillatory compound levels over the course of the 10 d experiment (Fig. 2 and *Table S1*). Another difference is the inherent heterogeneity of cancerous tissue. Some subpopulations of xenografted cells lie in closer proximity to newly formed blood vessels and hence may be more readily accessible to the drug than others (17, 18). Interactions with the host may also lead to additional complexity (19).

Comparison of the three genes that were most strongly affected in the in vivo experiment to their behavior in cell culture is of interest. Among the genes that were examined by qRT-PCR, *NPTX1* experienced the strongest in vivo repression (3.3-fold down). This was similar to the effects observed in cell culture, namely 2.6-fold and 3.5-fold repression at 48 h and 72 h, respectively. The effect of the Py-Im polyamide **1** against cells in culture was rather similar for both exposure times tested. By contrast, *SERPINE1* was less strongly affected in vivo compared to in vitro. While the in vivo repression amounted to 2.0-fold, the down-regulation was substantially more pronounced in cell culture. Transcription was reduced 8.3-fold after 48 h incubation and 15.7-fold after 72 h. Expression of *CCL2* was down-regulated 2.3-fold in the xenograft experiment whereas the cell culture repression was 2.2-fold (48 h) and 4.4-fold (72 h). This comparative analysis prompts a note of caution, for it is evident that there can be significant variability between gene expression changes observed in vitro and in vivo. We conclude, however, that cell culture data can be used to support in vivo findings in most cases.

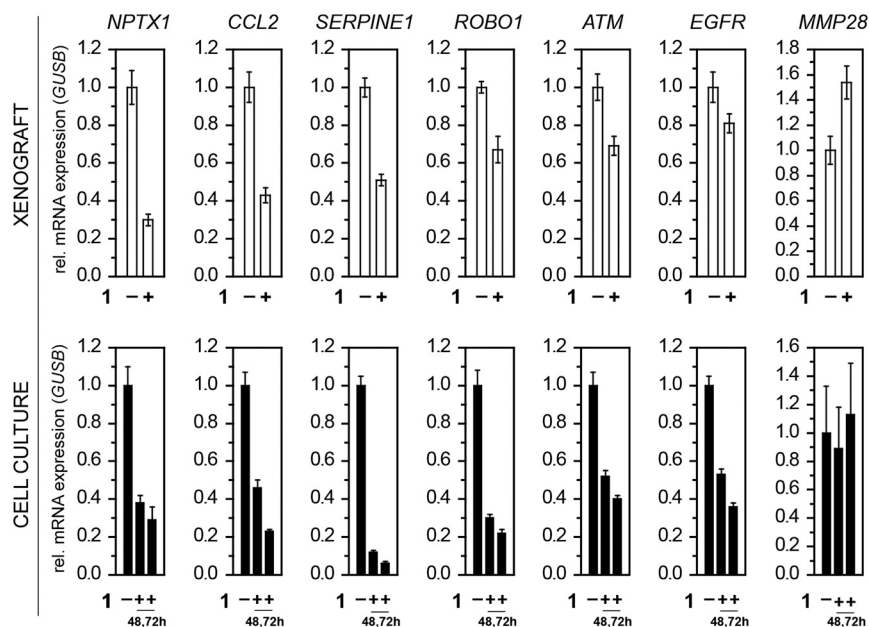


Fig. 5. A panel of genes affected by **1** in an A549-luc-C8 xenograft in SCID-bg animals (*Upper*) and cell culture (*Lower*). Xenograft: three independent experiments with $N = 5$ animals per treatment condition (vehicle vs **1**) were averaged. Cell culture: where indicated, the cells were incubated with Py-Im polyamide **1** at $10 \mu\text{M}$ final concentration in 0.1% DMSO as vehicle.

Tumor RNA-seq. Because of tumor heterogeneity, stemming mostly from host-derived tumor infiltrating cells, the fraction of sequencing reads unambiguously originating from the human transcriptome was at most only 60%, the rest being mouse-derived (see *SI Text*, Table S2). The computational pipeline described here solves this problem by applying simultaneous probabilistic mapping to both the human and the mouse transcriptome. Moreover, we have confirmed the viability of this approach by conducting qRT-PCR on a representative panel of genes, showing good correlation between the two methods (Table 1) and we expect it to be widely useful to researchers conducting similar types of experiments in different settings. Genome-wide analysis showed a total of 168 genes to be affected by the Py-Im polyamide **1** in xenografts, which corresponds to 0.76% of the NCBI reference sequence (refSeq) annotation ($p < 0.05$, at least twofold change). For comparison, Matsuda et al. reported gene expression changes in rat kidney cortex for 3% of genes interrogated by microarray (14).

Effects on Tumor Size. The tumor sizes were the same (within error) between the animal groups that received repeated injections of Py-Im polyamide **1** and vehicle (Fig. S3). The absence of any significant effect on tumor size could be due to a variety of fac-

tors. The compound might not reach sufficient average levels in the tumor. The IC_{50} value of **1** is $13 \pm 5 \mu\text{M}$ (Sulforhodamine B assay, 72 h incubation, 24 h recovery; see also *SI Text*, Fig. S1A). Although micromolar levels of **1** can be maintained for several hours postinjection, the overall exposure to the compound may still be too low to produce any measurable effect on size. Treatment efficiency could be enhanced by using more potent Py-Im polyamides or changing the route of administration, e.g., by employing osmotic pumps to maintain steady compound levels over the course of the experiment (20). Alternatively, Py-Im polyamide **1** may not penetrate the tumor to a sufficient depth because of tissue inhomogeneity. Tissue penetration rates can depend on compound lipophilicity and flexibility. Py-Im polyamide substituent variation affords a means to alter binding site preference, affinity, specificity, lipophilicity, and cellular uptake rates (21). Finally, the treatment schedule may be too short. Initial tumor growth is rather slow, the A549-luc-C8 tumors typically entering the exponential growth phase only several weeks after grafting (www.caliperls.com/assets/018/7635.pdf).

Conclusions

This study reports the ability of Py-Im polyamide **1** and its fluorescent labeled analogue **3** to traffic to the subcutaneously grafted A549-luc-C8 tumor. Unambiguous nuclear staining of tumor-derived cells with the FITC-analogue **3** evidenced the ability of the compound to remain at the site several days after injection. The nonfluorescent parent Py-Im polyamide **1** was capable of affecting gene expression in the tumor, and most trends correlated satisfactorily with cell culture data. From the panel of genes examined by qRT-PCR, the strongest effect was measured for *NPTX1*, which was repressed 3.3-fold. *MMP28* on the other hand experienced a small but significant induction of 1.5-fold upon treatment. It is of the highest importance to increase the potency of a compound at the tumor site, while minimizing its toxic effects to the host. Strategies to that end include testing of Py-Im polyamides targeted to different sequences, incorporating further modifications, development of formulations that would enhance selectivity of delivery and testing of alternative treatment schedules.

Table 1. Comparison of qRT-PCR and RNA-seq of A549-luc-C8 tumor xenograft gene expression levels normalized to GUSB as the housekeeping gene (qRT-PCR). Brackets indicate gene upregulation upon treatment. Three independent experiments with $N = 5$ animals per treatment condition (vehicle vs **1**) were averaged. RNA-seq was performed with single-end reads of 50 nt length. See *SI Text* for annotation of these gene products

Gene	Fold change (qPCR)	Fold change (RNA-seq)
<i>ATM</i>	1.5 ± 0.2	1.5 ($p > 0.05$)
<i>NPTX1</i>	3.3 ± 0.6	2.9 ($p < 0.001$)
<i>ROBO1</i>	1.5 ± 0.2	1.7 ($p > 0.05$)
<i>MMP28</i>	$[1.5 \pm 0.3]$	$[2.0]$ ($p < 0.05$)
<i>EGFR</i>	1.2 ± 0.2	1.3 ($p > 0.05$)
<i>CCL2</i>	2.3 ± 0.4	1.7 ($p < 0.001$)
<i>SERPINE1</i>	2.0 ± 0.2	1.8 ($p < 0.001$)

Materials and Methods

Polyamide Synthesis and Characterization. The polyamides 1–3 were synthesized following modified solid phase synthesis protocols (22). Typically, yields between 25 and 40% were observed. Compound purities were confirmed by analytical HPLC. Compounds 1 and 3 were characterized by MALDI-TOF MS as singly protonated species. Following masses were determined: 1 calculated for $C_{67}H_{79}N_{22}O_{13}$ $[M + H]^+$ 1,399.6, found 1,399.5; 3 calculated for $C_{80}H_{86}N_{23}O_{15}S$ $[M + H]^+$ 1,640.6, found 1,642.3. Analytical data for 2 were in agreement with what has been previously reported (10).

In Vitro Cell Culture Experiments. All experiments were conducted with A549-luc-C8 cells, unless specifically mentioned otherwise. Cells were grown in RPMI medium 1640, which was supplemented with 10% FBS and 1% penicillin/streptomycin, and did not exceed 25 passages. Confocal imaging, cellular proliferation and viability experiments as well as gene expression analyses by quantitative RT-PCR were performed following our previously published protocols (7, 10, 21, 23). Gene expression was normalized against *GUSB* as housekeeping gene. All primers yielded single amplicons as determined by both melting denaturation analysis and agarose gel electrophoresis. The following primer pairs were used. *CCL2*: fwd 5'-AGT GTC CCA AAG AAG CTG TGA-3' rev. 5'-AAT CCT GAA CCC ACT TCT GCT-3'; *SERPINE1*: fwd. 5'-AGA ACA GGA GGA GAA ACC CA-3' rev. 5'-AGC TCC TTG TAC AGA TGC CG-3'; *GUSB*: fwd. 5'-CTC ATT TGG AAT TTT GCC GAT T-3' rev. 5'-CCC AGT GAA GAT CCC CTT TTT A-3'; *ATM*: fwd. 5'-GCT GTG AGA AAA CCA TGG AA-3' rev. 5'-TTC AAA GGA TTC ATG GTC CAG-3'; *EGFR*: fwd. 5'-GGG CTC TGG AGG AAA AGA AA-3' rev. 5'-TCC TCT GGA GGC TGA GAA AA-3'; *MMP28*: fwd. 5'-CCT GCA GCT GCT ACT GTG G-3' rev. 5'-CTT TGG GGA CCT GTT CAT TG-3'; *NPTX1*: fwd. 5'-ACC GAG GAG AGG GTC AAG AT-3' rev. 5'-GTG GGA ATG TGA GCT GGA AC-3'; *ROBO1*: fwd. 5'-CAA TGC ATC GCT GGA AGT AG-3' rev. 5'-TTC TTC CAT GAA ATG GTG GG-3'.

Mouse Experiments. Pharmacokinetics. Analyses for Py-Im polyamide 1 were conducted following our recently established protocols (11). Briefly, the compound was injected subcutaneously into C57/Bl6 mice as a PBS/DMSO solution (4:1, 200 μ L per injection, four animals per group). Blood was collected retro-orbitally at the indicated time points. Plasma was obtained by centrifugation, precleared from protein by methanol precipitation and compound levels determined by analytical HPLC. The plasma levels obtained were compared with those previously reported for 2. **Xenografts. Grafting with A549-luc-C8.** Experiments were performed in female SCID-beige mice (Charles River) between 8 and 12 wk of age. Cells were injected into the left flank area of the animals as suspensions of 25×10^6 mL⁻¹ in RPMI, 200 μ L per injection. **Treatment and tumor proliferation monitoring.** Mice were treated

following the schedule delineated in *SI Text* (Table S1). Tumor proliferation was monitored using the XENOGEN imaging device. The animals were anesthetized with 2–5% isoflurane and subsequently transferred to the imaging chamber, whereupon the isoflurane levels were reduced to 1–2.5%. The floor of the imager was heated to +37 °C to avoid hypothermia. Breathing frequency was monitored and not allowed to drop below 1 s⁻¹, adjusting the isoflurane levels accordingly at all times. **Endpoint criteria and euthanasia.** Animal endpoint criteria encompassed weight loss of over 15%, restriction of motor function by the engrafted tumor, dehydration of over 10%, and moribund behavior. Where appropriate, the animals were euthanized by asphyxiation in a CO₂ chamber. **Tumor tissue harvest.** Animals were resected and tumors excised using standard forceps, scissors, and surgical blades. The tumors were combined into one sample per condition and mechanically sheared in TRIzol, employing a specialized device (tissue tearer, model 985370). Total RNA workup was performed following the standard TRIzol procedure, followed by a DNase digest.

RNA-seq Sample Preparation and Data Processing. Double polyA-selection was used in order to enrich for mRNA. RNA-seq libraries were prepared using standard Illumina reagents and protocols (24). All experiments were carried out in triplicate and 35 million–50 million single-end sequences of 50 bp were generated for each library. One replicate was additionally sequenced as 100 bp paired-end reads for quality control purposes. Sequencing data were mapped to a combined human and mouse transcriptome index (using the hg19 and mm9 refSeq annotations) using Bowtie version 0.12.7 (25) with two mismatches and an unlimited number of locations a read can map to. Alignments were quantified on the transcript level using eXpress 1.0.0 (bio.math.berkeley.edu/eXpress/index.html); for each gene the quantification values of all its transcripts were summed and the eXpress-determined “effective counts” were used as input for differential expression analysis using DESeq (16).

ACKNOWLEDGMENTS. J.A.R. is grateful to the Alexander von Humboldt foundation for the award of a Feodor Lynen postdoctoral fellowship. We thank Michael J. Waring for careful editing of the manuscript. N.G.N. would like to acknowledge the National Institutes of Health (NIH) and the Jonsson Cancer Center Foundation (JCCF) at UCLA for postdoctoral support. A.E.H. thanks the California Tobacco-Related Disease Research Program (19FT-0105) and the NIH (NRSA 1F32CA156833) for postdoctoral support. Sequencing was conducted at the Millard and Muriel Jacobs Genetics and Genomics Laboratory at California Institute of Technology. We are grateful for support by The Ellison Medical Foundation (AG-SS-2256-09) and the National Institutes of Health (GM051747).

- Dervan PB, Edelson BS (2003) Recognition of the DNA minor groove by pyrrole-imidazole polyamides. *Curr Opin Struct Biol* 13:284–299.
- Hsu CF, et al. (2007) Completion of a programmable DNA-binding small molecule library. *Tetrahedron* 63:6146–6151.
- White S, Szewczyk JW, Turner JM, Baird EE, Dervan PB (1998) Recognition of the four Watson-Crick base pairs in the DNA minor groove by synthetic ligands. *Nature* 391:468–471.
- Kielkopf CL, et al. (1998) A structural basis for recognition of A.T and T.A base pairs in the minor groove of B-DNA. *Science* 282:111–115.
- Chenoweth DM, Dervan PB (2009) Allosteric modulation of DNA by small molecules. *Proc Natl Acad Sci USA* 106:13175–13179.
- Edelson BS, et al. (2004) Influence of structural variation on nuclear localization of DNA-binding polyamide-fluorophore conjugates. *Nucleic Acids Res* 32:2802–2818.
- Nickols NG, Dervan PB (2007) Suppression of androgen receptor-mediated gene expression by a sequence-specific DNA-binding polyamide. *Proc Natl Acad Sci USA* 104:10418–10423.
- Olenyuk BZ, et al. (2004) Inhibition of vascular endothelial growth factor with a sequence-specific hypoxia response element antagonist. *Proc Natl Acad Sci USA* 101:16768–16773.
- Muzikar KA, Nickols NG, Dervan PB (2009) Repression of DNA-binding dependent glucocorticoid receptor-mediated gene expression. *Proc Natl Acad Sci USA* 106:16598–16603.
- Raskatov JA, et al. (2012) Modulation of NF- κ B-dependent gene transcription using programmable DNA minor groove binders. *Proc Natl Acad Sci USA* 109:1023–1028.
- Raskatov JA, Hargrove AE, So AY, Dervan PB (2012) Pharmacokinetics of Py-Im polyamides depend on architecture: Cyclic versus linear. *J Am Chem Soc* 134:7995–7999.
- Nagashima T, et al. (2009) Pharmacokinetic modeling and prediction of plasma pyrrole-imidazole polyamide concentration in rats using simultaneous urinary and biliary excretion data. *Biol Pharm Bull* 32:921–927.
- Matsuda H, et al. (2006) Development of gene silencing pyrrole-imidazole polyamide targeting the TGF- β 1 promoter for treatment of progressive renal diseases. *J Am Soc Nephrol* 17:422–432.
- Matsuda H, et al. (2011) Transcriptional inhibition of progressive renal disease by gene silencing pyrrole-imidazole polyamide targeting of the transforming growth factor- β 1 promoter. *Kidney Int* 79:46–56.
- Hargrove AE, Raskatov JA, Meier JL, Montgomery DC, Dervan PB (2012) Characterization and solubilization of pyrrole-imidazole polyamide aggregates. *J Med Chem* 55:5425–5432.
- Anders S, Huber W (2010) Differential expression analysis for sequence count data. *Genome Biol* 11:R106.
- Carmeliet P, Jain RK (2000) Angiogenesis in cancer and other diseases. *Nature* 407:249–257.
- Vaupel P, Kallinowski F, Okunieff P (1989) Blood-flow, oxygen and nutrient supply, and metabolic microenvironment of human-tumors—a review. *Cancer Res* 49:6449–6465.
- Bankert RB (2001) Human-SCID mouse chimeric models for the evaluation of anti-cancer therapies. *Trends Immunol* 22:386–393.
- Song P, et al. (2008) Activated cholinergic signaling provides a target in squamous cell lung carcinoma. *Cancer Res* 68:4693–4700.
- Meier JL, Montgomery DC, Dervan PB (2012) Enhancing the cellular uptake of Py-Im polyamides through next-generation aryl turns. *Nucleic Acids Res* 40:2345–2356.
- Puckett JW, Green JT, Dervan PB (2012) Microwave assisted synthesis of Py-Im polyamides. *Org Lett* 14:2774–2777.
- Nickols NG, Jacobs CS, Farkas ME, Dervan PB (2007) Improved nuclear localization of DNA-binding polyamides. *Nucleic Acids Res* 35:363–370.
- Mortazavi A, Williams BA, McCue K, Schaeffer L, Wold B (2008) Mapping and quantifying mammalian transcriptomes by RNA-Seq. *Nat Methods* 5:621–628.
- Langmead B, Trapnell C, Pop M, Salzberg SL (2009) Ultrafast and memory-efficient alignment of short DNA sequences to the human genome. *Genome Biol* 10:R25.